

Chapter 11

Recent Advances in Reaction-Diffusion Equations with Non-ideal Relays

Mark Curran, Pavel Gurevich and Sergey Tikhomirov

Abstract We survey recent results on reaction-diffusion equations with discontinuous hysteretic nonlinearities. We connect these equations with free boundary problems and introduce a related notion of spatial transversality for initial data and solutions. We assert that the equation with transverse initial data possesses a unique solution, which remains transverse for some time, and also describe its regularity. At a moment when the solution becomes nontransverse, we discretize the spatial variable and analyze the resulting lattice dynamical system with hysteresis. In particular, we discuss a new pattern formation mechanism—*rattling*, which indicates how one should reset the continuous model to make it well posed.

M. Curran (✉)
Institute of Mathematics I, Free University of Berlin, Arnimallee 7,
14195 Berlin, Germany
e-mail: mark.curran88@gmail.com

P. Gurevich
Institute of Mathematics I, Free University of Berlin, Arnimallee 3,
14195 Berlin, Germany
e-mail: gurevich@math.fu-berlin.de

P. Gurevich
Peoples' Friendship University of Russia, Miklukho-Maklaya Str. 6,
117198 Moscow, Russia

S. Tikhomirov
Max Planck Institute for Mathematics in the Sciences, Inselstraße 22,
04103 Leipzig, Germany
e-mail: sergey.tikhomirov@gmail.com

S. Tikhomirov
Chebyshev Laboratory, St. Petersburg State University, 14th Line, 29b,
199178 Saint Petersburg, Russia

11.1 Introduction

11.1.1 Motivation

In this chapter we will survey recent results on reaction-diffusion equations with a hysteretic discontinuity defined at every spatial point. We also refer to [1–3] and the more recent surveys by Visintin [4, 5] for other types of partial differential equations with hysteresis.

The equations we are dealing with in the present chapter were introduced in [6, 7] to describe growth patterns in colonies of bacteria (*Salmonella typhimurium*). In these experiments, bacteria (non-diffusing) are fixed to the surface of a petri dish, and their growth rate responds to changes in the relative concentrations of available nutrient and a growth-inhibiting by-product. The model asserts that at a location where there is a sufficiently high amount of nutrient relative to by-product, the bacteria will grow. This growth will continue until the production of by-product and diffusion of the nutrient lowers this ratio below a lower threshold, causing growth to stop. Growth will not resume until the diffusion of by-product raises the relative concentrations above an upper threshold that is distinct from the lower. Numerics in [6] reproduced the formation of distinctive concentric rings observed in experiments, however the question of the existence and uniqueness of solutions, as well as a thorough explanation of the mechanism of pattern formation, remained open.

Another application in developmental biology can be found, e.g., in [8], and an analysis of the corresponding stationary solutions in [9].

11.1.2 Setting of the Problem

In this chapter we will treat the following prototype problem:

$$u_t = \Delta u + f(u, v), \quad v = \mathcal{H}(\xi_0, u), \quad (x, t) \in Q_T, \tag{11.1}$$

$$u|_{t=0} = \varphi, \quad x \in Q, \tag{11.2}$$

$$\left. \frac{\partial u}{\partial \nu} \right|_{\partial' Q_T} = 0. \tag{11.3}$$

Here $Q \subset \mathbb{R}^n$ is a domain with smooth boundary, $Q_T := Q \times (0, T)$, where $T > 0$, $\partial' Q_T := \partial Q \times (0, T)$, u is a real-valued function on Q_T , and $\mathcal{H}(\xi_0, u)$ is a hysteresis operator defined as follows (see Fig. 11.1a). Fix two real numbers $\alpha < \beta$, an integer $\xi_0 \in \{-1, 1\}$, and two continuous functions $H_1 : (-\infty, \beta] \rightarrow \mathbb{R}$ and $H_{-1} : [\alpha, \infty) \rightarrow \mathbb{R}$ such that $H_1(u) \neq H_{-1}(u)$ for $u \in [\alpha, \beta]$. Define the sets

$$\Sigma_1 := \{(u, v) \in \mathbb{R}^2 \mid u \in (-\infty, \beta), v = H_1(u)\},$$

$$\Sigma_{-1} := \{(u, v) \in \mathbb{R}^2 \mid u \in (\alpha, \infty), v = H_{-1}(u)\}.$$

Definition 11.1.1 Let $u, v : [0, T] \rightarrow \mathbb{R}$, where u is a continuous function. We say that $v = \mathcal{H}(\xi_0, u)$ if the following hold:

1. $(u(t), v(t)) \in \Sigma_1 \cup \Sigma_{-1}$ for every $t \in [0, T]$.
2. If $u(0) \in (\alpha, \beta)$, then $v(0) = H_{\xi_0}(u(0))$.
3. If $u(t_0) \in (\alpha, \beta)$, then $v(t)$ is continuous in a neighborhood of t_0 .

The operator $\mathcal{H}(\xi_0, u)$ is called the *non-ideal relay* and item 3 means that the non-ideal relay jumps up (or down) when $u = \alpha$ (or $u = \beta$). This definition is equivalent to the definitions of non-ideal relay found in [1, 10, 11]. If $\mathcal{H}(\xi_0, u)(t) = H_j(u(t))$, then we call $\xi(t) := j$ the configuration of \mathcal{H} at the moment t , and we call ξ_0 the initial configuration. Now let $u : Q_T \rightarrow \mathbb{R}$ be a function of (x, t) and $\xi_0 : Q \rightarrow \{-1, 1\}$ a function of x , then $\mathcal{H}(\xi_0, u)(x, t)$ is defined in the same way by treating x as a parameter, i.e., there is a non-ideal relay at every $x \in Q$ with input $u(x, t)$, configuration $\xi(x, t)$, and initial configuration $\xi_0(x)$.

11.1.3 Set-Valued Hysteresis

First results on the well-posedness of (11.1)–(11.3) were obtained in [12, 13] for set-valued hysteresis, and their model problems are worth explaining in more detail. In both papers, the uniqueness of solutions as well as their continuous dependence on initial data remained open.

First we discuss the work of Visintin [13], which treats (11.1)–(11.3) for arbitrary $n \geq 1$ with $\mathcal{H}(\xi_0, u)$ replaced by a set-valued operator called a *completed relay* (see Fig. 11.1b). We still use the thresholds $\alpha < \beta$, and will consider constant hysteresis branches $H_1(u) \equiv 1$, and $H_{-1}(u) \equiv -1$. We also define the set $\Sigma_0 := \{(u, v) \in \mathbb{R}^2 \mid u \in [\alpha, \beta], v \in (-1, 1)\}$.

Definition 11.1.2 Let $u, v : [0, T] \rightarrow \mathbb{R}$, where u is a continuous function, and let $\xi_0 \in [-1, 1]$. We say $v \in \mathcal{H}_{\text{vis}}(\xi_0, u)$ if the following hold:

1. $(u(t), v(t)) \in \overline{\Sigma_1} \cup \overline{\Sigma_{-1}} \cup \Sigma_0$ for every $t \in [0, T]$.
2. If $u(0) \in (\alpha, \beta)$, then $v(0) = \xi_0$; if $u(0) = \alpha$ (or β), then $v(0) \in [\xi_0, 1]$ (or $v(0) \in [-1, \xi_0]$).

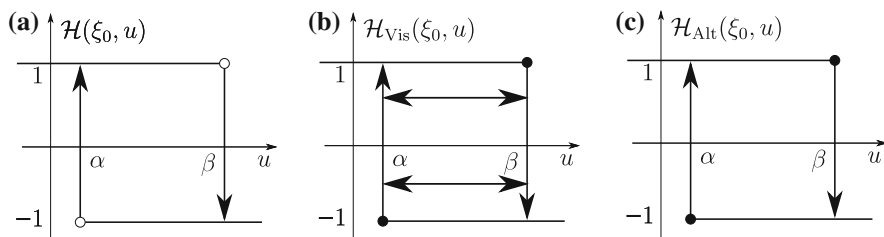


Fig. 11.1 The hysteresis operator with $H_1(u) \equiv 1$ and $H_{-1}(u) \equiv -1$

3. If $u(t_0) \in (\alpha, \beta)$, then $v(t)$ is constant in a neighborhood of t_0 .
4. If $u(t_0) = \alpha$ (or β), then $v(t)$ is non-decreasing (or non-increasing) in a neighborhood of t_0 .

By treating x as a parameter, $\mathcal{H}_{\text{Vis}}(\xi_0, u)$ is defined for $u : Q_T \rightarrow \mathbb{R}$ as we have done previously for $\mathcal{H}(\xi_0, u)$. Visintin [13] proved the existence of u and v such that the equation

$$u_t = \Delta u + v, \quad v \in \mathcal{H}_{\text{Vis}}(\xi_0, u),$$

with $n \geq 1$, Dirichlet boundary conditions, and initial data φ is satisfied in a weak sense in Q_T . Visintin [13] and more recently Aiki and Kopfova [14] proved the existence of solutions to modified versions of [6, 7], where the hysteretic discontinuity was a completed relay responding to a scalar input. A non-ideal relay with vector input, as in [6, 7], behaves almost identically to a non-ideal relay with scalar input, but for clarity of exposition we only consider scalar inputs in this chapter.

Let us now turn to the model hysteresis operator $\mathcal{H}_{\text{Alt}}(\xi_0, u)$ proposed by Alt in [12] (see Fig. 11.1c). We still consider $H_1(u) \equiv 1$ and $H_{-1}(u) \equiv -1$, and introduce the set

$$\tilde{\Sigma}_0 := \{(u, v) \in \mathbb{R}^2 \mid u = \alpha, v \in [-1, 1]\} \cup \{(u, v) \in \mathbb{R}^2 \mid u = \beta, v \in (-1, 1]\}.$$

Definition 11.1.3 Let $u, v : [0, T] \rightarrow \mathbb{R}$, where u is a continuous function, and let $\xi_0 \in \{-1, 1\}$. We say that $v \in \mathcal{H}_{\text{Alt}}(\xi_0, u)$ if the following hold:

1. $(u(t), v(t)) \in \Sigma_1 \cup \Sigma_{-1} \cup \tilde{\Sigma}_0$ for every $t \in [0, T]$.
2. If $u(0) \in [\alpha, \beta]$, then $v(0) = \xi_0$.
3. If $u(t_0) \in (\alpha, \beta)$, then $v(t)$ is constant in a neighborhood of t_0 .
4. If $u(t_0) = \alpha$ (or β), then $v(t)$ is non-decreasing (or non-increasing) in a neighborhood of t_0 .

One can define $\mathcal{H}_{\text{Alt}}(\xi_0, u)$ for $u : Q_T \rightarrow \mathbb{R}$ by treating x as a parameter as we did when defining $\mathcal{H}(\xi_0, u)$ and $\mathcal{H}_{\text{Vis}}(\xi_0, u)$.

To highlight the main difference between the completed relay $\mathcal{H}_{\text{Vis}}(\xi_0, u)$ and Alt’s relay $\mathcal{H}_{\text{Alt}}(\xi_0, u)$, suppose that $\mathcal{H}_{\text{Vis}}(\xi_0, u)(t_0), \mathcal{H}_{\text{Alt}}(\xi_0, u)(t_0) \in (-1, 1)$ and $u(t_0) = \beta$ has a local maximum at time t_0 . Then, as soon as u decreases, \mathcal{H}_{Alt} jumps to -1 , however \mathcal{H}_{Vis} remains constant.

Let us introduce the notation $\{u = \alpha\} := \{(x, t) \in \overline{Q_T} \mid u(x, t) = \alpha\}$, with $\{u = \beta\}$ defined analogously. Alt’s existence theorem can, omitting the technical assumptions, be stated in the following way. Let $n = 1$ and suppose $(\varphi, \xi_0) \in \overline{\Sigma_1} \cup \overline{\Sigma_{-1}}$. Then the following holds:

1. There exists u and v such that $v \in \mathcal{H}_{\text{Alt}}(\xi_0, u)$ a.e. in Q_T and

$$u_t = u_{xx} + v \quad \text{a.e. on } \{(x, t) \in Q_T \mid u(x, t) \notin \{\alpha, \beta\}\}.$$

2. We have

$$u_t = u_{xx} \quad \text{a.e. on } \{(x, t) \in Q_T \mid u(x, t) \in \{\alpha, \beta\}\},$$

$v \in [-1, 0]$ on $\{u = \beta\}$, and $v \in [0, 1]$ on $\{u = \alpha\}$.

3. Items 2–4 of Definition 11.1.3 hold in the following weak sense:

For every $\psi \in C_0^\infty(Q \times [0, T])$ with $\psi \geq 0$ on $\{Q \times [0, T]\} \cap \{u = \alpha\}$ and $\psi \leq 0$ on $\{Q \times [0, T]\} \cap \{u = \beta\}$,

$$\int_{Q_T} (v - v_0)\psi_t \, dxdt \leq 0.$$

11.1.4 Slow-Fast Approximation

Equations of the type (11.1)–(11.3) are deeply connected with slow-fast systems where the variable v is replaced by a fast bistable ordinary differential equation with a small parameter $\delta > 0$

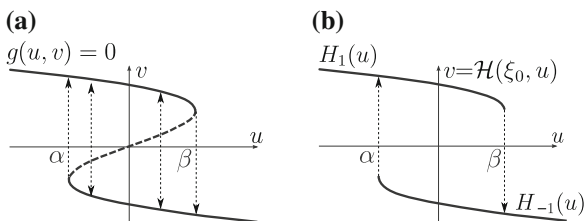
$$\delta v_t = g(u, v). \tag{11.4}$$

A typical example are the FitzHugh–Nagumo equations, where $g(u, v) = v - \frac{v^3}{3} - u$ and the hysteresis branches $H_1(u)$ and $H_{-1}(u)$ are the stable parts of the nullcline of g (see Fig. 11.2). The question of whether the hysteresis operator approximates the fast variable v as $\delta \rightarrow 0$ has been addressed for systems of ordinary differential equations (see, e.g., [15, 16] and further references in [17]), however the corresponding question for partial differential equations is still open.

11.1.5 Free Boundary Approach

Problem (11.1)–(11.3) with hysteresis has two distinct phases and a switching mechanism, hence it can be considered as a free boundary problem. First observe that the hysteresis \mathcal{H} naturally segregates the domain into two subdomains depending on the value of $\xi(x, t)$. Denote

Fig. 11.2 **a** The nullcline of the S -shaped nonlinearity $g(u, v)$. **b** Hysteresis with nonconstant branches $H_1(u)$ and $H_{-1}(u)$



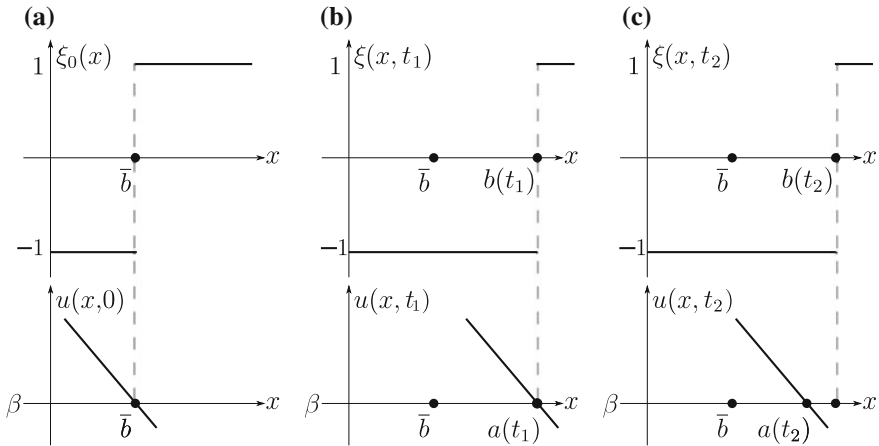


Fig. 11.3 An example of the hysteresis configuration ξ responding to an input u

$$Q_j := \{x \in Q \mid \xi_0(x) = j\}, \quad j = \pm 1. \tag{11.5}$$

Let us look at how the free boundary $\overline{Q_1} \cap \overline{Q_{-1}}$ can evolve for a simple example on the interval $Q = (0, 1)$. Consider a neighborhood U of $x \in Q$, and suppose at time $t = 0$, $Q_1 \cap U$ and $Q_{-1} \cap U$ are subintervals separated by a point $\bar{b} \in U$ (Fig. 11.3a). Let $u(x, t_0) > \beta$ for $x < \bar{b}$, $u(x, t_0) < \beta$ for $x > \bar{b}$, and let $x = a(t)$ be the unique solution of $u(x, t) = \beta$ in U . If at time $t_1 > 0$ the value of u at points $x > \bar{b}$ have already risen above β , then $\xi(x, t)$ has switched from 1 to -1 . These are the points x such that $\bar{b} < x \leq a(t_1)$ (Fig. 11.3b). Now if at time $t_2 > t_1$ the value of u at the switched points has fallen below β again, $\xi(x, t)$ remains switched. These are the points x such that $a(t_2) < x < a(t_1)$ (Fig. 11.3c). More succinctly, $\xi(x, t) = -1$ if $x \leq b(t)$ and $\xi(x, t) = 1$ if $x > b(t)$, where $b(t) = \max_{0 \leq s \leq t} a(s)$.

The point of this example is to illustrate that the free boundary does not in general coincide with the points where u is equal to one of the threshold values. This is different from the two-phase parabolic obstacle problem (see, e.g., [18, 19]), which (11.1)–(11.3) reduces to if $\alpha = \beta$.

Assume the derivative $\varphi'(\bar{b})$ in the above example was non-vanishing on the boundary $\{\bar{b}\} = \overline{Q_1} \cap \overline{Q_{-1}}$. This is an example of *transverse* initial data, and whether the initial data is transverse or not will play an important role in the analysis of problem (11.1)–(11.3).

11.1.6 Overview

This chapter is organized in the following way.

In Sect. 11.2 we will investigate the well-posedness of (11.1)–(11.3) for *transverse* initial data. For $n = 1$ the existence of solutions and their continuous dependence on initial data was established in [11], uniqueness of the solution in [20] and the analogous results for systems of equations in [21]. Preliminary results for $n \geq 2$ were obtained in [22].

In Sect. 11.3 we consider the regularity of solutions u , in particular, whether the generalized derivatives $u_{x_i x_j}$ and u_t are uniformly bounded. We will summarize the results of [23], where the authors proved that these derivatives are locally bounded in a neighborhood of a point not on the free boundary. They also showed that this bound depends on the parabolic distance to the parts of the free boundary that do not contain the sets $\{u = \alpha\}$ or $\{u = \beta\}$.

In Sect. 11.4 we consider non-transverse data and the results of [24]. We will analyze a spatio-temporal pattern (called *rattling*) arising after spatial discretization of the reaction-diffusion equation and discuss its connection with the continuous model with hysteresis operators \mathcal{H} , \mathcal{H}_{vis} , and \mathcal{H}_{Alt} .

11.2 Transverse Initial Data

11.2.1 Setting of a Model Problem

In this section we will discuss the well-posedness of problem (11.1)–(11.3) under the assumption that φ is transverse with respect to ξ_0 , a notion which we will make precise shortly. In order to illustrate the main ideas, we will treat the following model problem in detail and then discuss generalizations at the end of this section (see Sect. 11.2.4). Let $h_{-1} \leq 0 \leq h_1$ be two constants, and let the hysteresis branches be given by $H_1(u) \equiv h_1$ and $H_{-1}(u) \equiv h_{-1}$. Consider the prototype problem

$$u_t = \Delta u + \mathcal{H}(\xi_0, u), \quad (x, t) \in Q_T, \tag{11.6}$$

$$u|_{t=0} = \varphi, \quad x \in Q, \tag{11.7}$$

$$\frac{\partial u}{\partial \nu} \Big|_{\partial' Q_T} = 0. \tag{11.8}$$

We will treat $n = 1$ in Sect. 11.2.2 (see [11, 20]) and $n \geq 2$ (see [22]) in Sect. 11.2.3. Throughout this subsection we will always assume that φ and ξ_0 are *consistent* with each other, i.e., if $\varphi(x) < \alpha$ (or $\varphi(x) > \beta$), then $\xi_0(x) = 1$ (or $\xi_0(x) = -1$). In particular, this means that for every $x \in Q$, $\xi(x, t)$ is continuous from the right as a function of $t \in [0, T)$.

Since in general $\mathcal{H}(\xi_0, u) \in L_q(Q_T)$, we will look for solutions in the Sobolev space $W_q^{2,1}(Q_T)$ with $q > n + 2$. This is the space consisting of functions with two weak spatial derivatives and one weak time derivative from $L_q(Q_T)$ (see [25, Chap. 1]). If $u \in W_q^{2,1}(Q_T)$, then for every $t \in [0, T]$ the trace is well defined and

$u(\cdot, t) \in W_q^{2-2/q}(Q)$ (see, e.g., [25, p. 70]). To ensure that φ is regular enough to define the spatial transversality property, we henceforth fix a γ such that $0 < \gamma < 1 - (n + 2)/q$. It follows that if $\varphi \in W_q^{2-2/q}(Q)$, then $\varphi \in C^\gamma(\bar{Q})$ and $\nabla\varphi \in (C^\gamma(\bar{Q}))^n$, where C^γ is the standard Hölder space (see [26, Sect. 4.6.1]).

The subspace $W_{q,N}^{2-2/q}(Q) \subset W_q^{2-2/q}(Q)$ of functions with homogeneous Neumann boundary conditions is a well-defined subspace, and in this section we always assume that $\varphi \in W_{q,N}^{2-2/q}(Q)$.

Definition 11.2.1 A solution to problem (11.6)–(11.8) on the time interval $[0, T]$ is a function $u \in W_q^{2,1}(Q_T)$ such that (11.6) is satisfied in $L_q(Q_T)$ and u satisfies (11.7) and (11.8) in terms of traces. A solution on $[0, \infty)$ is a function $u : Q \times [0, \infty) \rightarrow \mathbb{R}$ such that for any $T > 0$, $u|_{Q_T}$ is a solution in the sense just described.

We note that if $u \in W_q^{2,1}(Q_T)$, then $\mathcal{H}(\xi_0, u)$ is a measurable function on Q_T (see [1, Sect. 6.1]).

11.2.2 Case $n = 1$

Let $Q = (0, 1)$ and Q_j be given by (11.5).

Definition 11.2.2 Let $\varphi \in C^1(\bar{Q})$. We say φ is *transverse* with respect to ξ_0 if the following hold:

1. There is a $\bar{b} \in (0, 1)$ such that $Q_{-1} = \{x \mid 0 \leq x \leq \bar{b}\}$ and $Q_1 = \{x \mid \bar{b} < x \leq 1\}$.
2. If $\varphi(\bar{b}) = \beta$, then $\varphi'(\bar{b}) < 0$.

An example of φ and ξ_0 satisfying Definition 11.2.2 is given in Fig. 11.3a.

Definition 11.2.3 A solution u is called *transverse* if for all $t \in [0, T]$, $u(\cdot, t)$ is transverse with respect to $\xi(\cdot, t)$.

Theorem 11.2.4 (See [11, Theorems 2.16 and 2.17]) *Suppose the initial data $\varphi \in W_{q,N}^{2-2/q}(Q)$ is transverse with respect to ξ_0 . Then there is a $T > 0$ such that the following hold:*

1. Any solution $u \in W_q^{2,1}(Q_T)$ of problem (11.6)–(11.8) is transverse.
2. There is at least one transverse solution $u \in W_q^{2,1}(Q_T)$ of problem (11.6)–(11.8).
3. If $u \in W_q^{2,1}(Q_T)$ is a transverse solution of problem (11.6)–(11.8), then it can be continued to a maximal interval of transverse existence $[0, T_{max})$, i.e., $u(x, T_{max})$ is not transverse or $T_{max} = \infty$.

We will sketch the proof of Theorem 11.2.4, part 2, assuming that $\varphi(\bar{b}) = \beta$ and $\varphi'(\bar{b}) < 0$.

Let us define the closed, convex, bounded subset of $C[0, T]$

$$B := \{b \in C[0, T] \mid b(t) \in [0, 1], b(0) = \bar{b}\}.$$

For any $b_0 \in B$, define the function

$$F(x, t) := \begin{cases} h_{-1} & \text{if } 0 \leq x \leq b_0(t), \\ h_1 & \text{if } b_0(t) < x \leq 1. \end{cases} \tag{11.9}$$

Let $u \in W_q^{2,1}(Q_T)$ be the solution to problem (11.6)–(11.8) with nonlinearity F in place of $\mathcal{H}(\xi_0, u)$. We claim that T can be chosen small enough such that the configuration $\xi(x, t)$ of $\mathcal{H}(\xi_0, u)$ is defined by a unique discontinuity point $b(t)$. Note that we do not yet claim that $F = \mathcal{H}(\xi_0, u)$.

To prove the claim, first fix $T_0 > 0$. It is a result of classical parabolic theory [25, Chap. 4] that for all $T \in [0, T_0]$

$$\|u\|_{C^\nu(\overline{Q_T})} + \|u_x\|_{C^\nu(\overline{Q_T})} \leq C_1 \left(\|F\|_{L_q(Q_T)} + \|\varphi\|_{W_{q,N}^{2-2/q}(Q)} \right) \leq C_2, \tag{11.10}$$

where $C_1, C_2, \dots > 0$ depend only on T_0 and q . The claim now follows from (11.10) with the help of the implicit function theorem.

Observe that u is a solution of problem (11.6)–(11.8) if $\mathcal{H}(\xi_0, u) = F$, i.e., $b_0 = b$. We therefore look for a fixed point of the map $\mathcal{R} : B \rightarrow B$, $\mathcal{R}(b_0) := b$.

Consider $b_{01}, b_{02} \in B$ and define F_1, F_2 via b_{01}, b_{02} similarly to (11.9), and let u_1, u_2 be the corresponding solutions. Observe that $F_1 \neq F_2$ only if

$$\min(b_{01}(t), b_{02}(t)) < x < \max(b_{01}(t), b_{02}(t)),$$

in particular,

$$\begin{aligned} \|u_1 - u_2\|_{C^\nu(\overline{Q_T})} + \|u_{1x} - u_{2x}\|_{C^\nu(\overline{Q_T})} &\leq C_1 \|F_1 - F_2\|_{L_q(Q_T)}, \\ &\leq C_3 \|b_{01} - b_{02}\|_{C[0,T]}^{1/q}. \end{aligned} \tag{11.11}$$

Applying (11.10) again, and using $\varphi'(\bar{b}) > 0$ and the implicit function theorem, we see that the left hand side of (11.11) bounds $\|a_1 - a_2\|_{C[0,T]}$. One can additionally show that $\|a_1 - a_2\|_{C[0,T]}$ bounds $\|b_1 - b_2\|_{C[0,T]}$, hence

$$\|b_1 - b_2\|_{C[0,T]} \leq \|a_1 - a_2\|_{C[0,T]} \leq C_4 \|b_{01} - b_{02}\|_{C[0,T]}^{1/q}. \tag{11.12}$$

In particular (11.12) shows that \mathcal{R} is a continuous map on B . Moreover, one can use (11.10) to show that $\mathcal{R}(B)$ is bounded in $C^\nu[0, T]$, and since $C^\nu[0, T]$ is compactly embedded into $C[0, T]$, the Schauder fixed point theorem implies that \mathcal{R} has a fixed point.

Theorem 11.2.5 (see [20, Theorem 2.2]) *If u_1 and u_2 are transverse solutions of problem (11.6)–(11.8) with the same φ , then $u_1 \equiv u_2$.*

We prove the theorem by expressing solutions as a convolution with the Green function $G(x, y, t, s)$ for the heat equation with Neumann boundary conditions.

Let us use this function to estimate the solution $w = u_1 - u_2$ of the heat equation with zero initial data, Neumann boundary conditions, and the right hand side $h = \mathcal{H}(\xi_0, u_1) - \mathcal{H}(\xi_0, u_2)$:

$$|w(x, t)| \leq \int_0^t \int_Q |G(x, y, t, s)| |h(y, s)| dy ds. \tag{11.13}$$

Also note that G satisfies the inequality (see, e.g., [27])

$$|G(x, y, t, s)| \leq \frac{C_1}{(t - s)^{1/2}}, \quad x, y \in Q, \quad 0 \leq s < t, \tag{11.14}$$

where $C_1 > 0$ does not depend on x, y, t or s .

Similarly to the proof of Theorem 11.2.4, for every $s \leq t$ the integral of $|h(y, s)|$ over Q is bounded by $\|b_1 - b_2\|_{C[0,t]}$ and hence by $\|a_1 - a_2\|_{C[0,t]}$ and hence by $\|u_1 - u_2\|_{C(\overline{Q}_T)}$. Combining this with (11.13) and (11.14), and taking the supremum over $(x, t) \in Q_T$ we get

$$\|w\|_{C(\overline{Q}_T)} \leq C_2 \sqrt{T} \|w\|_{C(\overline{Q}_T)},$$

where $C_2 > 0$ does not depend on T . Thus $w = 0$ for T small enough. A passage to arbitrary T is standard.

Theorem 11.2.6 (See [11, Theorem 2.9]) *Let $u \in W_q^{2,1}(Q_T)$ be a transverse solution of problem (11.6)–(11.8). If $\|\varphi - \varphi_n\|_{W_q^{2-2/q}(Q)} \rightarrow 0$ and $|\bar{b}_n - \bar{b}| \rightarrow 0$ as $n \rightarrow \infty$, then for sufficiently large n , problem (11.6)–(11.8) has a solution $u_n \in W_q^{2,1}(Q_T)$ with initial data φ_n and initial configuration ξ_{0n} defined via \bar{b}_n . Furthermore, $\|u_n - u\|_{W_q^{2,1}(Q_T)} \rightarrow 0$ as $n \rightarrow \infty$.*

The crux of the proof is showing that for sufficiently large n , all the solutions exist on the same time interval $[0, T]$. To this end we note that we have in fact given an explicit construction of T , and that this T depends on \bar{b} , $\|\varphi\|_{W_q^{2-2/q}(Q)}$, and if $\varphi(\bar{b}) = \beta$, also on $\varphi'(\bar{b})$. Hence for φ_n and \bar{b}_n close enough to φ and \bar{b} in their respective norms, the same T can be used.

11.2.3 Case $n \geq 2$

For the case $n \geq 2$ a notion of transversality has been studied in a model problem. For clarity we will define transversality for the case where the threshold β is adjoined to the free boundary between Q_1 and Q_{-1} , and α is not. In what follows, let $\text{int}(A)$ denote the topological interior of a subset $A \subset Q$, and let $\{\varphi = \alpha\}$ be defined similarly to $\{u = \alpha\}$ but taking $x \in \overline{Q}$ instead of $(x, t) \in \overline{Q}_T$. In [22] the existence and

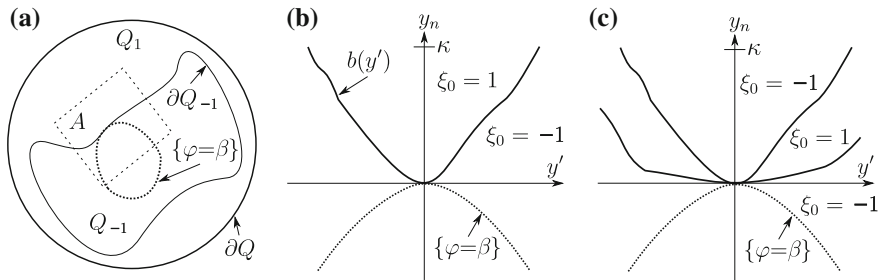


Fig. 11.4 An example of **a** the sets $Q_{\pm 1}$, **b** transverse data, and **c** non-transverse data

uniqueness of solutions were studied for initial data transverse in the following sense (see Fig. 11.4a, b, and recall that Q_j is given by (11.5)).

Definition 11.2.7 We say the function φ is transverse with respect to ξ_0 if the following hold:

1. Q_1 and Q_{-1} are measurable, $\partial Q_{-1} \subset Q$, $\partial Q_1 = \partial Q_{-1} \cup \partial Q$, and ∂Q_{-1} has zero Lebesgue measure.
2. $\varphi(x) < \beta$ for $x \in \text{int}(Q_1) \cup \partial Q$.
3. $\varphi(x) > \alpha$ for $x \in Q_{-1}$.
4. If $x \in \{u = \beta\} \cap \partial Q_{-1}$, then there is a neighbourhood A of x , a set $A' \subset \mathbb{R}^{n-1}$, a $\kappa > 0$, and a map ψ such that

(a) ψ is a composition of a translation and a rotation, and

$$\psi(A) = A' \times [-\kappa, \kappa], \quad \psi(x) = (0, 0).$$

(b) There is a continuous function $\bar{b} : A' \rightarrow [-\kappa, \kappa]$ such that the configuration function $\xi_0 \circ \psi^{-1}$ in $\psi(A)$ (which we denote by $\xi_0(y', y_n)$, $y' \in A'$) is given by

$$\xi_0(y', y_n) = \begin{cases} -1 & \text{if } -\kappa \leq y_n \leq \bar{b}(y'), \\ 1 & \text{if } \bar{b}(y') < y_n \leq \kappa. \end{cases}$$

(c) $\varphi \circ \psi^{-1}$, which we write as $\varphi(y', y_n)$, satisfies $\varphi_{y_n}(0, 0) < 0$.

We observe that in Sect. 11.2.2, the boundary between Q_1 and Q_{-1} was a single point \bar{b} . But when $n \geq 2$, this boundary is assumed to have the structure of a continuous codimension 1 submanifold in a neighborhood of a point on the free boundary where φ takes a threshold value. Also note that for $n \geq 2$ non-transversality can be caused by the geometry of ∂Q_{-1} in addition to the possible degeneracy of $\nabla \varphi$ (see Fig. 11.4c and Sect. 11.2.4 for further discussion).

Theorem 11.2.8 (see [22, Theorems 3.18 and 3.19]) *Assume that $n \geq 2$ and $\varphi \in W_{q,N}^{2-2/q}(Q)$ is transverse with respect to ξ_0 . Then there is a $T > 0$ such that any*

solution $u \in W_q^{2,1}(Q_T)$ to problem (11.6)–(11.8) is transverse and there is at least one such solution. Moreover, if for some $T' > 0$, u_1 and u_2 are two transverse solutions to problem (11.6)–(11.8) on $Q_{T'}$, then $u_1 \equiv u_2$.

The main ideas of the proof are similar to those for the case $n = 1$. Since $(\varphi(y', \cdot), \xi_0(y', \cdot))$ is transverse in the 1d sense for every $y' \in A'$, one can prove continuity of a map \mathcal{R} that now maps functions $u_0 \in C^\lambda(\overline{Q_T})$ ($\lambda < \gamma$) to solutions $\mathcal{R}(u_0) := u$ of problem (11.6)–(11.8) with the right hand side $\mathcal{H}(\xi_0, u_0)$. Estimate (11.10) implies that $u \in C^\gamma(\overline{Q_T})$, and the compactness of the embedding $C^\gamma(\overline{Q_T}) \subset C^\lambda(\overline{Q_T})$ and the Schauder fixed point theorem together imply that \mathcal{R} has a fixed point in $C^\gamma(\overline{Q_T})$.

11.2.4 Generalizations and Open Problems

Let us list some generalizations for the case $n = 1$.

Change of topology. Suppose $u(x, t)$ becomes non-transverse at some time T in the sense of Definition 11.2.2. Then one of two possibilities arise. Either $u(x, T)$ has touched a threshold with zero spatial derivative at some point in $(0, 1)$, or this is not the case but $\lim_{t \rightarrow T} b(t) = 1$. In the latter case, one can continue the solution, and it remains unique, by redefining the problem effectively without hysteresis [11, Theorem 2.18]. We say that the topology of the hysteresis has changed at time T , in the sense that ξ transitions from piecewise constant to uniformly constant.

Continuous dependence on initial data. If u is a solution such that the topology has changed for some $t_1 < T$, then u need not continuously depend on the initial data since a sequence of approximating solutions u_n may become non-transverse at moments τ_n with $\tau_n < t_1$ and $\lim_{n \rightarrow \infty} \tau_n = t_1$ (the dashed line in Fig. 11.5). But

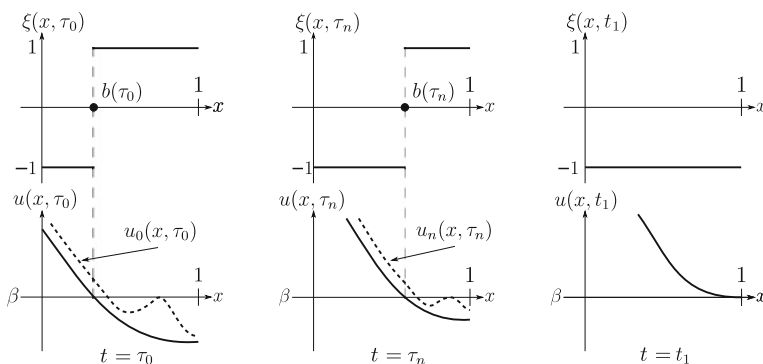


Fig. 11.5 A solution u (drawn as solid lines in the lower picture) and its configuration ξ (the upper picture) that remain transverse as a discontinuity of ξ disappears at time t_1 . The dashed line in the lower picture is a series of non-transverse approximations u_n that become non-transverse at moments τ_n with $\tau_n < t_1$ and $\lim_{n \rightarrow \infty} \tau_n = t_1$

if we also assume that each u_n is a transverse solution, then solutions do depend continuously on their initial data.

Finite number of discontinuities. The results in Sect. 11.2.2 remain valid if the hysteresis topology is defined by finitely many discontinuity points. The hysteresis changing topology in the sense we described for one point of discontinuity corresponds to these points merging together in the general case (see Fig. 11.6).

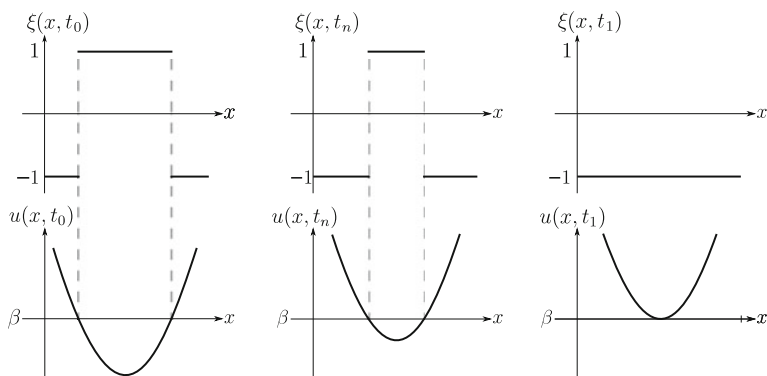


Fig. 11.6 Discontinuities merging as $t \rightarrow t_1$

General nonlinearity. The results in this section also hold for the more general problem (11.1)–(11.3). First one must assume that f is locally Lipschitz and dissipative (see [11, Condition 2.11]). With such an f , and if H_1 and H_{-1} are locally Hölder continuous, then transverse solutions exist and can be continued up to a maximal interval of transverse existence. If one additionally assumes that transverse solutions are unique, they can be shown to continuously depend on their initial data. To prove the uniqueness of solutions the authors of [20, 22] make the stronger assumption on H_1 and H_{-1} , namely that

$$|H_1(u_1) - H_1(u_2)| \leq \frac{M}{(\beta - u_1)^\sigma + (\beta - u_2)^\sigma} |u_1 - u_2|,$$

for u_1, u_2 in a left neighborhood of β , with $M > 0$ and $\sigma \in (0, 1)$, plus an analogous inequality for H_{-1} and a right neighborhood of α . This condition covers the case where H_1 and H_{-1} are the stable branches in the slow-fast approximation as in Fig. 11.2 (see the appendix of [20] for further discussion).

Systems of equations. In [21, Theorem 2.1], the results of Sect. 11.2.2 were generalized to systems of equations of the type in problem (11.1)–(11.3). It was also shown therein that problem (11.1)–(11.3) can be coupled to ordinary differential equations to cover the Hoppensteadt–Jäger model from [6, 7].

Let us conclude this subsection by discussing an open problem.

Open problem. In Fig. 11.4c, one can see that for every $y' \neq 0$, $(\varphi(y', \cdot), \xi_0(y', \cdot))$ is transverse in the 1d sense (with two discontinuities), but since the free boundary

cannot be represented as a graph with codomain y_n at the point $y' = 0$, this initial data is not transverse. Whether Definition 11.2.7 can be generalized to include such cases is the subject of future work, and at this stage the authors strongly suspect that item 4 of Definition 11.2.7 can be replaced by the following statement: *if $x \in \{u = \beta\} \cap \partial Q_{-1}$, then $\nabla\varphi(x) \neq 0$* . In other words, the assumption that the free boundary is a graph is not necessary, and hence Fig. 11.4c would also be transverse. This question is intimately linked to the topology of the free boundary. Whether solutions can be continued to a maximal interval of existence and how to pose continuous dependence of initial data is unclear for the quite general conditions on Q_{-1} and Q_1 in Definition 11.2.7. These questions also apply to the case where $n = 1$ and ξ_0 has infinitely many discontinuities.

11.3 Regularity of Strong Solutions

To begin with let us discuss what we mean by regularity of solutions in this context. First observe that we cannot expect a classical solution since \mathcal{H} has a jump discontinuity. Therefore the “optimal” regularity we expect is $W_\infty^{2,1}$. In this section we obtain $W_\infty^{2,1}$ “locally”, for points $(x, t) \in Q_T$ outside of the static part of the free boundary. We will also assume the following condition:

Condition 11.3.1 $H_1(u) \equiv 1$ and $H_{-1}(u) \equiv -1$.

Let us introduce the notation $Q_T^{\pm 1} := \{(x, t) \mid \xi(x, t) = \pm 1\}$ and observe that u is smooth on the interior of $Q_T^{\pm 1}$.

The free boundary is defined as the set $\Gamma := \partial Q_T^1 \cap \partial Q_T^{-1}$. Moreover, we define $\Gamma_\alpha := \{u = \alpha\} \cap \Gamma$ and $\Gamma_\beta := \{u = \beta\} \cap \Gamma$. Note that both Γ_α and Γ_β have zero Lebesgue measure whenever u is a solution of problem (11.6)–(11.8). This follows from the fact that $u_t - \Delta u = 0$ a.e. on $\Gamma_\alpha \cup \Gamma_\beta$ and Condition 11.3.1 (see Alt’s argument in the introduction and [12]).

The estimates we obtain will depend critically on the *static* part of the free boundary $\Gamma_v := \Gamma \setminus (\Gamma_\alpha \cup \Gamma_\beta)$. If $(x, t) \in \Gamma_v$, then $u(x, t) \neq \alpha, \beta$ and by continuity of u , $u(x, t \pm \tau) \neq \alpha, \beta$ for τ sufficiently small. This means $\xi(x, t \pm \tau) = \xi(x, t)$ and so if we draw the t -axis vertically as in Fig. 11.7, Γ_v looks like a vertical strip.

Next we recall the definition of a parabolic cylinder

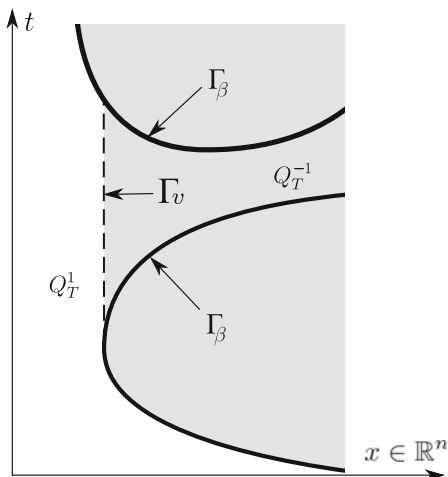
$$P_r(x^0, t^0) := \{x \in \mathbb{R}^n \mid \|x^0 - x\|_{\mathbb{R}^n} < r\} \times (t^0 - r^2, t^0 + r^2), \quad r > 0.$$

We define the parabolic distance between (x^0, t^0) and a set $A \subset Q_T$ as

$$\text{dist}_p((x^0, t^0), A) := \sup\{r > 0 \mid P_r(x^0, t^0) \cap \{t \leq t^0\} \cap A = \emptyset\}.$$

This is all the notation we need to state the main result of [23].

Fig. 11.7 A possible scenario where $\Gamma \neq \Gamma_\alpha \cup \Gamma_\beta$ and Γ_v appears. White and grey indicate the regions Q_T^1 and Q_T^{-1} respectively



Theorem 11.3.2 (see [23, Theorem 2.3]) *We assume that $n \geq 1$ and u is a solution of problem (11.6)–(11.8). Then*

$$|u_t(x, t)| + \sum_{i,j=1}^n |u_{x_i x_j}(x, t)| \leq C(\rho_v, \rho_b, M), \quad \text{a.e. } (x, t) \in Q_T \setminus \overline{\Gamma_v},$$

where C depends on $\rho_v := \text{dist}_p((x, t), \Gamma_v)$, $\rho_b := \text{dist}_p((x, t), \partial' Q_T \cup (Q \times \{0\}))$, and $M := \sup_{(x,t) \in Q_T} |u(x, t)|$.

To explain the main ideas in the proof we define some further notation. Let $\Gamma_\alpha^0 = \Gamma_\alpha \cap \{\nabla u = 0\}$ and $\Gamma_\alpha^* = \Gamma_\alpha \setminus \Gamma_\alpha^0$, with Γ_β^0 and Γ_β^* defined similarly. Furthermore, define $\Gamma^0 = \Gamma_\alpha^0 \cup \Gamma_\beta^0$ and $\Gamma^* = \Gamma_\alpha^* \cup \Gamma_\beta^*$.

The crucial point in the proof is the quadratic growth estimate

$$\sup_{P_r(x,t)} |u - \beta| \leq C_1(\rho_v, \rho_b, M)r^2 \quad \text{for } r \leq \min\{\rho_v, \rho_b\}, \tag{11.15}$$

and $(x, t) \in \Gamma_\beta^0$ (the estimate on Γ_α^0 is similar). The main tool for showing the quadratic bound (11.15) is the local rescaled version of the Caffarelli monotonicity formula, see [23, 28, 29].

Furthermore, the quadratic growth estimate (11.15) implies the corresponding linear bound for $|\nabla u|$

$$\sup_{P_r(x,t)} |\nabla u| \leq C_2(\rho_v, \rho_b, M)r \quad \text{for all } r \leq \min\{\rho_v, \rho_b\}, \tag{11.16}$$

with $(x, t) \in \Gamma^0$. The dependence of C_1 and C_2 on the distance ρ_v in (11.15) and (11.16) arises due to the monotonicity formula. Near Γ_v neither the local rescaled

version of Caffarelli’s monotonicity formula nor its generalizations (such as the almost monotonicity formula) are applicable to the positive and negative parts of the spatial directional derivatives $D_e u$, with $e \in \mathbb{R}^n$.

Besides estimates (11.15) and (11.16), one also needs information about the behaviour of u_t near Γ^* . Although u_t may have jumps across the free boundary, one can show that u_t is a continuous function in a neighborhood of $(x, t) \in \Gamma^* \setminus \Gamma_\nu$. In addition, the monotonicity of the jumps of $\mathcal{H}(\xi_0, u)$ in the t -direction provides one-sided estimates of u_t near Γ_α and Γ_β . Combining these results with the observation that $u_t \leq 0$ on $\Gamma_\alpha^* \setminus \Gamma_\nu$, and $u_t \geq 0$ on $\Gamma_\beta^* \setminus \Gamma_\nu$ gives

$$\sup_{\Gamma^* \setminus \Gamma_\nu} |u_t| \leq C_3(\rho_b, M). \tag{11.17}$$

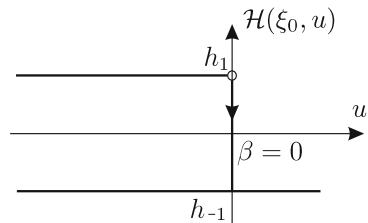
Inequalities (11.15)–(11.17) allow one to apply methods from the theory of free boundary problems (see, e.g., [18, 19]) and estimate $|u_t(x, t)|$ and $|u_{x_i x_j}(x, t)|$ for a.e. $(x, t) \in Q_T \setminus \overline{\Gamma_\nu}$.

11.4 Non-transverse Initial Data

11.4.1 Setting of a Problem

In this section we summarize the recent work [24], where the nontransverse case is analyzed for $x \in \mathbb{R}$, and indicate directions for further research. We will be interested in the behavior of solutions near one of the thresholds, say β . Therefore, we set $\alpha = -\infty$ and $\beta = 0$ (see Fig. 11.8) and assume that the initial data satisfy $\varphi(x) = -cx^2 + o(x^2)$ in a small neighborhood of the origin, $\varphi(x) < 0$ everywhere outside of the origin, $\xi_0(x) = -1$ for $x = 0$, and $\xi_0(x) = 1$ for $x \neq 0$. In particular, we assume $c > 0$. In this situation, the theorems in Sect. 11.2.2 are not applicable. Hence, to understand the dynamics of the solution near the origin, we approximate the continuous equation (11.6) by its spatial discretization and the initial data by the discrete quadratic function. Namely, we choose a grid step $\varepsilon > 0$, set $u_n^\varepsilon(t) := u(\varepsilon n, t)$, $n \in \mathbb{Z}$, and consider the system of infinitely many ordinary differential equations with hysteresis

Fig. 11.8 Hysteresis with thresholds $\alpha = -\infty$ and $\beta = 0$



$$\frac{du_n^\varepsilon}{dt} = \frac{u_{n+1}^\varepsilon - 2u_n^\varepsilon + u_{n-1}^\varepsilon}{\varepsilon^2} + \mathcal{H}(u_n^\varepsilon), \quad t > 0, \quad n \in \mathbb{Z}, \tag{11.18}$$

supplemented by the nontransverse (quadratic) initial data

$$u_n^\varepsilon(0) = -c(\varepsilon n)^2, \quad n \in \mathbb{Z}. \tag{11.19}$$

Here we do not explicitly indicate the dependence of \mathcal{H} on ξ_0 , assuming that $\mathcal{H}(u_n^\varepsilon)(t) = h_1$ if $u_n^\varepsilon(s) < 0$ for all $s \in [0, t]$ and $\mathcal{H}(u_n^\varepsilon)(t) = h_{-1}$ otherwise. As before, we assume that $h_{-1} \leq 0 < h_1$.

Due to [24, Theorem 2.5], problem (11.18), (11.19) admits a unique solution in the class of functions satisfying

$$\sup_{s \in [0, t]} |u_n^\varepsilon(s)| \leq A e^{B|n|}, \quad n \in \mathbb{Z}, \quad t \geq 0,$$

with some $A = A(t, \varepsilon) \geq 0$ and $B = B(t, \varepsilon) \in \mathbb{R}$. Thus, we are now in a position to discuss the dynamics of solutions for each fixed grid step ε and analyze the limit $\varepsilon \rightarrow 0$.

First, we observe that ε in (11.18), (11.19) can be scaled out. Indeed, setting

$$u_n(t) := \varepsilon^{-2} u_n^\varepsilon(\varepsilon^2 t) \tag{11.20}$$

reduces problem (11.18), (11.19) to the equivalent one

$$\begin{cases} \frac{du_n}{dt} = u_{n+1} - 2u_n + u_{n-1} + \mathcal{H}(u_n), & t > 0, \quad n \in \mathbb{Z}, \\ u_n(0) = -cn^2, & n \in \mathbb{Z}. \end{cases} \tag{11.21}$$

Using the comparison principle, it is easy to see that if $h_1 \leq 2c$, then $u_n(t) < 0$ for all $n \in \mathbb{Z}$ and $t > 0$ and, therefore, no switchings happen for $t > 0$. Let us assume that

$$h_{-1} \leq 0 < 2c < h_1. \tag{11.22}$$

It is easy to show that $u_n(t) \leq 0$ for all $n \in \mathbb{Z}$ and $t > 0$. However, some nodes can now reach the threshold $\beta = 0$ and switch the hysteresis. The main question is which nodes do this and according to which law.

11.4.2 Numerical Observations

The following pattern formation behavior is indicated by numerics (see Fig. 11.9). As time goes on, the spatial profile of $u_n(t)$ forms two symmetric hills propagating away from the origin. At the same time, the whole spatial profile oscillates up and

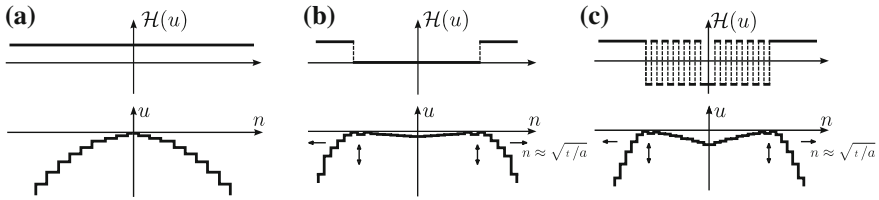


Fig. 11.9 Upper graphs represent spatial profiles of the hysteresis $\mathcal{H}(u_n)$ and lower graphs the spatial profiles of the solution u_n . **a** Nontransverse initial data. **b** Spatial profiles at a moment $t > 0$ for $h_{-1} = 0$. **c** Spatial profiles at a moment $t > 0$ for $h_{-1} = -h_1 < 0$

down (never exceeding the threshold $\beta = 0$) and touches the threshold $\beta = 0$ in such a way that

$$\lim_{j \rightarrow \infty} \frac{N_{ns}(j)}{N_s(j)} = \frac{|h_{-1}|}{h_1}, \tag{11.23}$$

where $N_s(j)$ and $N_{ns}(j)$ are integers denoting the number of nodes in the set $\{u_0, u_{\pm 1}, \dots, u_{\pm j}\}$ that switch and do not switch, respectively, on the time interval $[0, \infty)$. In [24], such a spatio-temporal pattern was called *rattling*.

A more specific pattern occurs if $|h_{-1}|/h_1 = p_{ns}/p_s$, where p_s and p_{ns} are co-prime integers. In this case, for any j large enough, the set $\{u_{j+1}, \dots, u_{j+p_s+p_{ns}}\}$ contains exactly p_s nodes that switch and p_{ns} nodes that do not switch on the time interval $[0, \infty)$.

If a node u_n switches on the time interval $[0, \infty)$, then we denote its switching moment by t_n ; otherwise, set $t_n := \infty$. In particular, finite values of t_n characterize the propagation velocity of the two hills mentioned above. Numerics indicates that, for the nodes where t_n is finite, we have

$$t_n = an^2 + \begin{cases} O(\sqrt{n}) & \text{if } h_{-1} = 0, \\ O(n) & \text{if } h_{-1} < 0, \end{cases} \quad \text{as } n \rightarrow \infty, \tag{11.24}$$

and

$$|u_{k+1}(t) - u_k(t)| \leq b, \quad |k| \leq n, \quad t \geq t_n, \quad n = 0, 1, 2, \dots, \tag{11.25}$$

where $a, b > 0$ do not depend on k and n . In particular, (11.24) and (11.25) mean that the hills propagate with velocity of order $t^{-1/2}$, while the cavity between the hills has a bounded steepness, which distinguishes the observed phenomenon from the ‘‘classical’’ traveling wave situation.

11.4.3 Rigorous Result

The recent work [24] provides a rigorous analysis of the rattling in the case $h_{-1} = 0$, where, according to (11.24), all the nodes are supposed to switch at time moments satisfying

$$t_n = an^2 + q_n, \quad |q_n| \leq E\sqrt{n}, \tag{11.26}$$

where $E > 0$ does not depend on $n \in \mathbb{Z}$. In [24], the authors found the coefficient a and proved that if finitely many nodes $u_n(t)$, $n = 0, \pm 1, \dots, \pm n_0$, switch at time moments t_n satisfying (11.26), then all the nodes $u_n(t)$, $n \in \mathbb{Z}$, switch at time moments t_n satisfying (11.26) (see the rigorous statement below). One of the main tools in the analysis is the so-called discrete Green function $y_n(t)$ that is a solution of the problem

$$\begin{cases} \dot{y}_0 = \Delta y_0 + 1, & t > 0, \\ \dot{y}_n = \Delta y_n, & t > 0, \quad n \neq 0, \\ y_n(0) = 0, & n \in \mathbb{Z}. \end{cases} \tag{11.27}$$

The important property of the discrete Green function is the following asymptotics proved in [30]:

$$y_n(t) = \sqrt{t} f\left(\frac{|n|}{\sqrt{t}}\right) + O\left(\frac{1}{\sqrt{t}}\right) \quad \text{as } t \rightarrow \infty, \tag{11.28}$$

where

$$f(x) := 2x \int_x^\infty \mathbb{Z}^{-2} h(\mathbb{Z}) d\mathbb{Z}, \quad h(x) := \frac{1}{2\sqrt{\pi}} e^{-\frac{x^2}{4}}, \tag{11.29}$$

and $O(\cdot)$ does not depend on $n \in \mathbb{Z}$.

Now if we (inductively) assume that the nodes $u_0, u_{\pm 1}, \dots, u_{\pm(n-1)}$ switched at the moments satisfying (11.26), while no other nodes switched on the time interval $[0, t_{n-1}]$, then the dynamics of the node

$u_n(t)$ for $t \geq t_{n-1}$ (and until the next switching in the system occurs) is given by

$$u_n(t) = -cn^2 + (h_1 - 2c)t - h_1 \sum_{k=-(n-1)}^{n-1} y_{n-k}(t - t_k). \tag{11.30}$$

At the (potential) switching moment $t_n = an^2 + q_n$, the relations $t_k = ak^2 + q_k$ ($|k| \leq n - 1$), equality (11.30), the Taylor formula, and asymptotics (11.28) yield

$$\begin{aligned}
 0 &= -cn^2 + (h_1 - 2c)an^2 - h_1 \sum_{k=-(n-1)}^{n-1} y_{n-k} \left(a(n^2 - k^2) \right) + \text{l.o.t.} \\
 &= -cn^2 + (h_1 - 2c)an^2 - h_1 \sum_{k=-(n-1)}^{n-1} \sqrt{a(n^2 - k^2)} f\left(\frac{n - k}{\sqrt{a(n^2 - k^2)}} \right) \quad (11.31) \\
 &+ \text{l.o.t.} \\
 &= (-c + (h_1 - 2c)a - h_1 R_n(a)) n^2 + \text{l.o.t.},
 \end{aligned}$$

where

$$R_n(a) := \sum_{k=-(n-1)}^{n-1} \frac{1}{n} \sqrt{a(1 - (k/n)^2)} f\left(\frac{1 - k/n}{\sqrt{a(1 - (k/n)^2)}} \right)$$

and ‘‘l.o.t.’’ stands for lower order terms that we do not explicitly specify here. Note that $R_n(a)$ is the Riemann sum for the integral

$$I_f(a) := \int_{-1}^1 \sqrt{a(1 - x^2)} f\left(\frac{1 - x}{\sqrt{a(1 - x^2)}} \right) dx. \quad (11.32)$$

Therefore, equality (11.31) can be rewritten as

$$0 = (-c + (h_1 - 2c)a - h_1 I_f(a)) n^2 + \text{l.o.t.} \quad (11.33)$$

It is proved in [24] that there exists a unique $a > 0$ for which the coefficient at n^2 in (11.33) vanishes. The most difficult part is to analyze the lower order terms in (11.33) that involve:

1. the remainders $q_0, q_{\pm 1}, \dots, q_n$ from (11.26) arising from (11.30) via the application of the Taylor formula,
2. the remainder in the asymptotic (11.28) for the discrete Green function $y_n(t)$,
3. the remainders arising from approximating the integral $I_f(a)$ by the Riemann sum $R_n(a)$.

In particular, one has to prove that if $|q_j| \leq E\sqrt{|j|}$ for $j = 0, \pm 1, \dots, \pm(n - 1)$, then the lower order terms vanish for a specified above and $|q_n| \leq E\sqrt{|n|}$. This allows one to continue the inductive scheme and (after an appropriate analysis of the nodes $u_{\pm(n+1)}(t), u_{\pm(n+2)}(t), \dots$ for $t \in [t_{n-1}, t_n]$) complete the proof.

The rigorous formulation of the main result in [24] is as follows.

Theorem 11.4.1 (see [24, Theorem 3.2]) *Assume that (11.22) holds and that $h_{-1} = 0$. Let $a = a(h_1/c) > 0$ be a (unique) root of the equation*

$$-c + (h_1 - 2c)a - h_1 I_f(a) = 0 \quad (11.34)$$

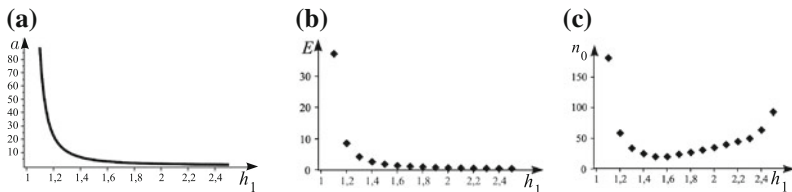


Fig. 11.10 Dependence on h_1 of the values of a , E , and $n_0(E)$ that fulfill assumptions (11.35) for $c = 1/2$. **a** The values of a are found as roots of (11.34). **b, c** The values of E and $n_0(E)$ are calculated for discrete values $h_1 = 1.1, 1.2, 1.3, \dots, 2.5$

with $I_f(a)$ given by (11.32). Then there exists a constant $E_0 = E_0(h_1, c, a) > 0$ and a function $n_0 = n_0(E) = n_0(E, h_1, c, a)$ (both explicitly constructed) with the following property. If

$$\begin{aligned} & \text{finitely many nodes } u_0(t), u_1(t), \dots, u_{n_0}(t) \text{ switch at moments } t_n \\ & \text{satisfying (11.26) with the above } a \text{ and some } E \geq E_0, \end{aligned} \tag{11.35}$$

then each node $u_n(t)$, $n \in \mathbb{Z}$, switches; moreover, the switching occurs at a time moment t_n satisfying (11.26) with a and E as in (11.35).

We note that the explicit formula (11.30) for the solution $u_n(t)$ allows one to verify the fulfillment of finitely many assumptions (11.35) numerically with an arbitrary accuracy for any given values of h_1 and c . The graphs in Fig. 11.10 taken from [24] represent the values of a , E , and $n_0(E)$ that fulfill assumption (11.35) for $c = 1/2$ and $h_1 = 1.1, 1.2, 1.3, \dots, 2.5$.

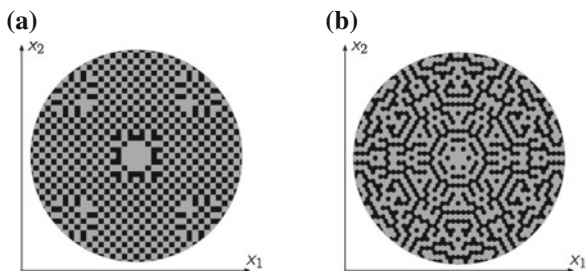


Fig. 11.11 A snapshot for a time moment $t > 0$ of a two-dimensional spatial profile of hysteresis taking values $h_1 > 2c > 0$ and $h_{-1} = -h_1 < 0$. The nontransverse initial data is given by $\varphi(x) = -c(x_1^2 + x_2^2)$. Grey (black) squares or hexagons correspond to the nodes that have (not) switched on the time interval $[0, t]$. **a** Discretization on the square lattice. **b** Discretization on the triangular lattice

11.4.4 Open Problems

To conclude this section, we indicate several directions of further research in the nontransverse case.

Case $h_{-1} < 0$. In this case, one has to additionally prove a specific switching pattern (11.23). We expect that the tools developed in [24] will work for rational h_1/h_{-1} . The irrational case appears to be a much more difficult problem.

Multi-dimensional case. Numerics indicates that the behavior analogous to (11.23) occurs in higher spatial dimensions for different kinds of approximating grids. Figure 11.11 illustrates the switching pattern for a two-dimensional analog of problem (11.21), where the Laplacian is discretized on the square and triangular lattices, respectively.

Limit $\varepsilon \rightarrow 0$. We introduce the function

$$u^\varepsilon(x, t) := u_n^\varepsilon(t), \quad x \in [\varepsilon n - \varepsilon/2, \varepsilon n + \varepsilon/2), \quad n \in \mathbb{Z},$$

(which is piecewise constant in x for every fixed t). Making the transformation inverse to (11.20) and assuming (11.23) and (11.24), we can deduce that, as $\varepsilon \rightarrow 0$, the function $u^\varepsilon(x, t)$ approximates a smooth function $u(x, t)$, which satisfies $u(x, t) = 0$ for $x \in (-\sqrt{t/a}, \sqrt{t/a})$. In other words, $u(x, t)$ sticks to the threshold line $\beta = 0$ on the expanding interval $x \in (-\sqrt{t/a}, \sqrt{t/a})$.

Similarly to $u^\varepsilon(x, t)$, we consider the function

$$H^\varepsilon(x, t) := \mathcal{H}(u_n^\varepsilon)(t), \quad x \in [\varepsilon n - \varepsilon/2, \varepsilon n + \varepsilon/2), \quad n \in \mathbb{Z},$$

which is supposed to approximate the hysteresis $\mathcal{H}(u)(x, t)$ in (11.6). We see that the spatial profile of $H^\varepsilon(x, t)$ for $x \in (-\sqrt{t/a}, \sqrt{t/a})$ is a step-like function taking values h_1 and h_{-1} on alternating intervals of length of order ε . Hence, it has no pointwise limit as $\varepsilon \rightarrow 0$, but converges in a weak sense to the function $H(x, t)$ given by $H(x, t) = 0$ for $x \in (-\sqrt{t/a}, \sqrt{t/a})$ and $H(x, t) = h_1$ for $x \notin (-\sqrt{t/a}, \sqrt{t/a})$. We emphasize that $H(x, t)$ does not depend on h_{-1} (because a does not). On the other hand, if $h_{-1} < 0$, the hysteresis operator $\mathcal{H}(u)(x, t)$ in (11.6) cannot take value 0 by definition, which clarifies the essential difficulty with the well-posedness of the original problem (11.6) in the nontransverse case. To overcome the non-wellposedness, one need to allow the intermediate value 0 for the hysteresis operator, cf. the discussion of modified hysteresis operators due to Visintin and Alt in the introduction. A rigorous analysis of the limit $\varepsilon \rightarrow 0$ is an open problem, which may lead to a unique “physical” choice of an appropriate element in the multi-valued Visintin’s hysteresis $\mathcal{H}_{\text{vis}}(\xi_0, u)$ in Definition 11.1.2.

Rattling in slow-fast systems. One may think that the rattling occurs exclusively due to the discontinuous nature or hysteresis. This is not quite the case. Consider an equation of type (11.6) with the hysteresis $\mathcal{H}(\xi_0, u)$ replaced by the solution v of a bistable ordinary differential equation of type (11.4), e.g.,

$$u_t = u_{xx} + v, \quad \delta v_t = g(u, v). \tag{11.36}$$

Numerical solution of system (11.36) with a nontransverse initial data $u(x, 0) = -cx^2 + o(x^2)$ and $v(x, 0) = H_1(\beta)$ near the origin reveals a behavior analogous to that for a spatially discrete system (see Fig. 11.12). As the spatial profile of $u(x, t)$ touches the threshold β at some point x_0 , the spatial profile of $v(x, t)$ forms a peak-like transition layer around x_0 that rapidly converges to a plateau. Thus, as time goes on, the spatial profile of $v(x, t)$ converges to a step-like function taking values $H_1(\beta)$ and $H_{-1}(\beta)$ on alternating intervals, whose length tends to zero as $\delta \rightarrow 0$. A rigorous analysis of the limit $\delta \rightarrow 0$ is an open problem.

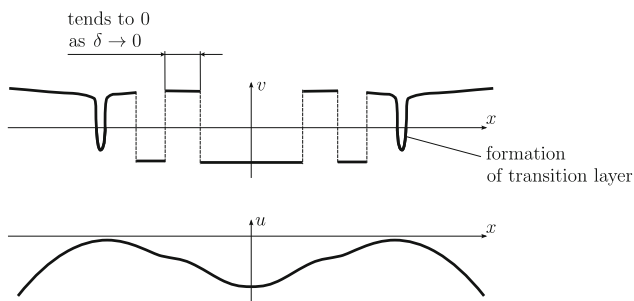


Fig. 11.12 Lower and upper graphs are spatial profiles of the solution $u(x, t)$ and $v(x, t)$, respectively, for problem (11.36) with initial data $u|_{t=0} = -cx^2 + o(x^2)$, $v|_{t=0} = H_1(\beta)$

Acknowledgments The authors are grateful for the support of the DFG project SFB 910 and the DAAD project G-RISC. The work of the first author was partially supported by the Berlin Mathematical School. The work of the second author was partially supported by the DFG Heisenberg programme. The work of the third author was partially supported by Chebyshev Laboratory (Department of Mathematics and Mechanics, St. Petersburg State University) under RF Government grant 11.G34.31.0026, JSC ‘‘Gazprom neft’’, by the Saint-Petersburg State University research grant 6.38.223.2014 and RFBR 15-01-03797a.

References

1. A. Visintin, *Differential Models of Hysteresis*. Applied Mathematical Sciences (Springer-Verlag, Berlin, 1994)
2. P. Krejčí, *Hysteresis Convexity and Dissipation in Hyperbolic Equations*. GAKUTO International series (Gattōtoscho, 1996)
3. M. Brokate, J. Sprekels, *Hysteresis and Phase Transitions*. Applied Mathematical Sciences (Springer-Verlag, New York, 1996)
4. A. Visintin, *Acta Applicandae Mathematicae* **132**(1), 635 (2014)
5. A. Visintin, *Discrete Contin. Dyn. Syst.*, Ser. S **8**(4), 793 (2015)
6. F. Hoppensteadt, W. Jäger, in *Biological Growth and Spread. Lecture Notes in Biomathematics*, vol. 38, ed. by W. Jäger, H. Rost, P. Tautu (Springer, Berlin Heidelberg, 1980), pp. 68–81

7. F. Hoppensteadt, W. Jäger, C. Pöppe, in *Modelling of Patterns, in Space and Time. Lecture Notes in Biomathematics*, ed. by W. Jäger, J.D. Murray (Springer, Berlin Heidelberg, 1984), vol. 55, pp. 123–134
8. A. Marciniak-Czochra, *Math. Biosci.* **199**(1), 97 (2006)
9. A. Köthe, Hysteresis-driven pattern formation in reaction-diffusion-ode models. Ph.D. thesis, University of Heidelberg (2013)
10. M. Krasnosel'skii, M. Niezgodka, A. Pokrovskii, *Systems with Hysteresis* (Springer, Berlin, 2012)
11. P. Gurevich, S. Tikhomirov, R. Shamin, *SIAM J. Math. Anal.* **45**(3), 1328 (2013)
12. H.W. Alt, *Control Cybern.* **14**(1–3), 171 (1985)
13. A. Visintin, *SIAM J. Math. Anal.* **17**(5) (1986)
14. T. Aiki, J. Kopfová, in *Recent Advances in Nonlinear Analysis* (2008), pp. 1–10
15. P. Krejčí, *J. Physics.: Conf. Ser.* (22), 103 (2005)
16. E. Mischenko, N. Rozov, *Differential Equations with Small Parameters and Relaxation Oscillations* (Plenum, New York, 1980)
17. C. Kuehn, *Multiple Time Scale Dynamics, Applied Mathematical Sciences*, vol. 191 (Springer International Publishing, 2015)
18. D. Apushkinskaya, N. Uraltseva, *St. Petersburg. Math. J.* **25**(2), 195 (2014)
19. H. Shahgholian, N. Uraltseva, G.S. Weiss, *Adv. Math.* **221**(3), 861 (2009)
20. P. Gurevich, S. Tikhomirov, *Nonlinear Anal.* **75**(18), 6610 (2012)
21. P. Gurevich, S. Tikhomirov, *Mathematica Bohemica (Proc. Equadiff 2013)* **139**(2), 239 (2014)
22. M. Curran, Local well-posedness of a reaction-diffusion equation with hysteresis. Master's thesis, Fachbereich Mathematik und Informatik, Freie Universität Berlin (2014)
23. D. Apushkinskaya, N. Uraltseva, *Interfaces and Free Boundaries* **17**(1), 93 (2015)
24. P. Gurevich, S. Tikhomirov, [arXiv:1504.02385](https://arxiv.org/abs/1504.02385) [math.AP] (2015)
25. O. Ladyzhenskaya, V. Solonnikov, N. Uraltseva, *Linear and Quasilinear Equations of Parabolic Type* (American Mathematical Society, Providence, Rhode Island, 1968)
26. H. Triebel, *Interpolation Theory, Function Spaces, Differential Operators*. Carnegie-Rochester Conference Series on Public Policy (North-Holland Publishing Company, 1978)
27. S. Ivasishen, *Math. USSR-Sb* (4), 461 (1981)
28. L. Caffarelli, S. Salsa, *A Geometric Approach to Free Boundary Problems*. Graduate Studies in Mathematics (American Mathematical Soc., 2005)
29. D. Apushkinskaya, H. Shahgholian, N. Uraltseva, *J. Math. Sci.* **115**(6), 2720 (2003)
30. P. Gurevich, [arXiv:1504.02673](https://arxiv.org/abs/1504.02673) [math.AP] (2015)